Anisotropy-Induced Quantum Interference and Population Trapping Between Orthogonal Quantum Dot Exciton States in Semiconductor Cavity Systems

Stephen Hughes[1] and Girish Agarwal[2,3]

[1]*Department of Physics, Queen's University, Kingston, Ontario, Canada, K7L 3N6*
[2]*Institute for Quantum Science and Engineering and Department of Biological and Agricultural Engineering,*
Texas A&M University, College Station, Texas 77845
[3]*Department of Physics, Oklahoma State University, Stillwater, OK 74078, USA*
(Dated: July 4, 2018)

We describe how quantum dot semiconductor cavity systems can be engineered to realize anisotropy-induced dipole-dipole coupling between orthogonal dipole states in a single quantum dot. Quantum dots in single-mode cavity structures as well as photonic crystal waveguides coupled to spin states or linearly polarized excitons are considered. We demonstrate pronounced dipole-dipole coupling to control the radiative decay rate of excitons and form pure entangled states in the long time limit. We investigate both field-free entanglement evolution and coherently pumped exciton regimes, and show how a double pumping scenario can completely eliminate the decay of coherent Rabi oscillations and lead to population trapping. In the Mollow regime, we explore the emitted spectra from the driven dipoles and show how a non-pumped dipole can take on the form of a spectral triplet, quintuplet, or a singlet, which has applications for producing subnatural linewidth single photons and more easily accessing regimes of high-field quantum optics and cavity-QED.

Introduction. The ability to manipulate spontaneous emission (SE) decay and coherent coupling between quantum dipoles is a key requirement for many applications in quantum optics, including the creation of entangled photon sources and qubit entanglers. Quantum dots (QDs) are especially preferable for studying quantum optical effects due to the large transition dipole moments. A major problem with entangling excitons from spatially separated QDs is due to their large inhomogeneous broadening, leading to negligible photon-coupling rates. In 2000, Agarwal [1] showed how vacuum-induced interference effects from an anisotropic vacuum can lead to quantum interference effects among decay channels of closely lying states, even though the dipoles are orthogonal: *anisotropic vacuum-induced interference* (AVI). Subsequently, there have been several related theoretical works, though no reported experiments to our knowledge. Li *at al.* [2] demonstrated AVI using a 3-level atom in a multilayered dielectric medium. Recently, Jha *et al.* [3] studied a QD coupled to a metamaterial surface to predict AVI using nanoantenna designs, which has the potential advantage of remote distance control; the AVI was shown to allow a maximum population transfer between the orthogonal dipoles of around 1%, and similar proposals have been later reported by Sun and Jiang [4]. While interesting, these studies are difficult to realize experimentally, and the predicted population transfer coupling effects are rather weak. Moreover, the plasmonic systems introduce material losses [5], and large Purcell factor regimes would be necessary in general.

In practical QD systems, large radiative decay rates are required and more easily achieved in semiconductor nanophotonic systems. For efficient single photon β factors, slow-light PC waveguides have been shown to yield almost perfect single photons on-chip [6]; such waveguides also exhibit a rich polarization dependence, including points of linear and circular polarization. Charge neutral QD excitons in general exhibit either linear polarization or circular polarization if the fine structure splitting (FSS) is negligible [7–9], which can now be controlled with great precision [10]. Charged QD excitons can also be used to study interactions between single spins and photons [11], which is important for quantum networks. It would thus be highly desirable to study and exploit AVI effects in such geometries, using realistic QD exciton states. Moreover, one would like to go beyond the free-field case of vacuum dynamics and study field-driven coupling via a pump field where such effects can be more easily accessed and exploited experimentally. Suppressing SE in QDs shows good promise for low error rate quantum logic operations [12], and previous attempts to do this are difficult and limited, e.g., using photonic crystal (PC) bandgaps [13]; in addition, the coherent generation of subnatural light from QDs has applications for single photon sources [14], and allows one to more easily access interesting strong field physics.

In this Letter, we introduce several practical, and experimentally feasible, QD photonic systems that can enable and exploit pronounced AVI, causing long lived entangled photon states with an almost perfect means of achieving population transfer and population trapping—a feat that is not possible with spatially separated QD dipoles. Figure 1 shows a schematic of QD exciton states and example photonic systems including a microcavity with a linearly-polarized cavity mode, and a PC waveguide that exhibits linear to circular polarization on the
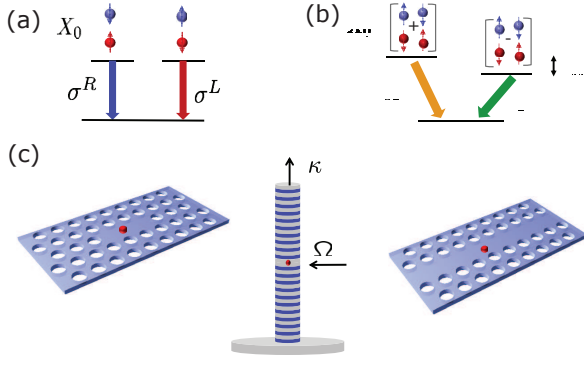
FIG. 1: Example QD states, (a) left/right circularly polarized or (b) X/Y linearly polarized, using neutral exciton states that can be coupled engineered field modes in a nanophotonic system. The dipole directions are in the plane, caused by stronger quantum confinement in the vertical direction, and the neutral dot excitons may also be split by a small fine structure splitting (FSS). (c) Selection of microcavity and waveguide systems where the field polarization can be controlled, also showing an example of external pumping.

so-called L lines (or X points) and C points, respectively [15, 16]. Such systems provide a high degree of anisotropy needed for observing AVI using QDs. Our significant findings are: (i) AVI produces long lived entangled QD states with a population transfer which is orders of magnitude larger than in other systems, (ii) coherent pumping with two pump fields creates a population trapping state in the form of a pure Bell entangled state, and (iii) selective pumping of the transitions enables one to study features of Mollow triplets which are strictly due to AVI, e.g., where one excited dipole acts as the pump for the other dipole and long lives Rabi oscillations can be coherently controlled with great precision.

Theory. Photon transfer can be rigorously modelled through the the electric-field Green function, $\mathbf{G}(\mathbf{r}, \mathbf{r}'; \omega)$ which describes the field response at $\mathbf{r}$ to a point source at $\mathbf{r}'$ where $\mathbf{G}_{i,j}$ is a second rank tensor. Planar PC waveguide modes below the light line ($\omega = c|\mathbf{k}|$) will propagate without loss through an ideal structure (neglecting imperfections) and can be written as $\mathbf{f}_{k_\omega}(\mathbf{r}) = \sqrt{\frac{a}{L}}\mathbf{e}_{k_\omega}(\mathbf{r})e^{ik_\omega x}$, where $\mathbf{e}_{k_\omega}(\mathbf{r})$ is the Bloch mode, sharing the same periodicity as the lattice, a is the pitch of the PC, and L is the length of the structure; $\mathbf{e}_{k_\omega}(\mathbf{r})$ is normalized from $\int_{V_c} \epsilon(\mathbf{r})\mathbf{e}_{k_\omega}(\mathbf{r}) \cdot \mathbf{e}_{k'_\omega}^*(\mathbf{r}') = \delta_{k_\omega, k'_\omega}$, where V_c is the spatial volume of a PC unit-cell. The waveguide Green function can be obtained analytically [17, 18],

$$\mathbf{G}_{\mathrm{wg}}(\mathbf{r}, \mathbf{r}'; \omega) = \frac{ia\omega}{2v_g}\Big[\Theta(x - x')\mathbf{e}_{k_\omega}(\mathbf{r})\mathbf{e}_{k_\omega}^*(\mathbf{r}')e^{ik_\omega(x-x')}$$
$$+ \Theta(x' - x)\mathbf{e}_{k_\omega}^*(\mathbf{r})\mathbf{e}_{k_\omega}(\mathbf{r}')e^{ik_\omega(x'-x)}\Big], \quad (1)$$

where the terms preceded by Heaviside functions correspond to forward and backwards propagating modes, respectively, and v_g is the group velocity at the frequency on interest. To account for coupling to other modes,

one can simply add other terms to the total Green function, though these are typically negligible in comparison to contribution from slow-light Bloch modes. For a single mode cavity system, with resonant frequency ω_c and mode profile, $\mathbf{f}_c(\mathbf{r})$, the cavity Green function is

$$\mathbf{G}_c(\mathbf{r}, \mathbf{r}'; \omega) \approx \frac{\omega^2 \mathbf{f}_c(\mathbf{r})\mathbf{f}_c^*(\mathbf{r}')}{\omega^2 - \omega_c^2 - i\omega\Gamma_c}, \quad (2)$$

where at a field antinode the modes can be normalized through $|\mathbf{f}_c(\mathbf{r}_0)|^2 = \eta(\mathbf{r})/V_{\mathrm{eff}}\varepsilon_b$, with ε_b the background effective index and $\eta(\mathbf{r})$ accounts for any deviations from the mode antinode position and polarization.

Working in a rotating frame with respect to a laser frequency ω_L, we derive the quantum master equation (ME) for the QD interacting with a general photonic reservoir. In the weak-coupling regime, with the system-reservoir coupling given by the dipole interaction in the rotating-wave approximation, we apply the second-order Born and Markov approximations to the interaction Hamiltonian, and trace out the photon bath [19–21]. Thus, the waveguide and microcavity systems considered in this work, the coupling rates are assumed to be in the weak-coupling regime. Defining $\sigma_{\alpha\beta} = |\alpha\rangle\langle\beta|$, $\alpha, \beta = g, a, b$, the ME is

$$\dot{\rho} = i\sum_{n=a,b}\Delta\omega_n[\sigma_{nn}, \rho] + i\sum_{n,n'}^{n\neq n'}\delta_{n,n'}[\sigma_{ng}\sigma_{gn'}, \rho]$$
$$+ \sum_{n,n'}\Gamma_{n,n'}\left(\sigma_{gn'}\rho\sigma_{ng} - \frac{1}{2}\{\sigma_{ng}\sigma_{gn'}, \rho\}\right) - \frac{i}{\hbar}[H_{\mathrm{P}}, \rho]$$
$$+ \sum_n \gamma_n'\mathcal{L}[\sigma_{nn}], \quad (3)$$

where $n = a, b; n' = a, b$ for two excitons at a QD position $\mathbf{r}_0$, $\Delta\omega_n = (\omega_L - \omega_n')$, $\omega_n' = \omega_n - \Delta_n$, and $\Delta_n = \frac{1}{\hbar\epsilon_0}\mathbf{d}_n^\dagger \cdot \mathrm{Re}\{\mathbf{G}(\mathbf{r}_0, \mathbf{r}_0; \omega_n)\} \cdot \mathbf{d}_n$ is the photonic Lamb shift; $H_{\mathrm{P}} = \sum_{n=a,b}\frac{\hbar\Omega_n}{2}(\sigma_{gn} + \sigma_{ng})$ models a possible external coherent drive applied to each dipole, with an effective Rabi field $\Omega_n = \langle\hat{\mathbf{E}}_{\mathrm{pump},n}(\mathbf{r}_n) \cdot \mathbf{d}_n\rangle/\hbar$ [22]; and γ_n' models a pure dephasing process. Note that this ME (3) is more general than the one in [1], and we also include coupling through the real part of the Green function, fully accounting for photon exchange through both real and virtual photons. The dipole-dipole coupling terms and radiative decay rates are [33]

$$\delta_{n,n'}|_{n\neq n'} = \frac{1}{\hbar\epsilon_0}\mathrm{Re}\left[\mathbf{d}_n^\dagger \cdot \mathbf{G}(\mathbf{r}_0, \mathbf{r}_0; \omega_{n'}') \cdot \mathbf{d}_{n'}\right], \quad (4)$$

$$\Gamma_{n,n'} = \frac{2}{\hbar\epsilon_0}\mathrm{Im}\left[\mathbf{d}_n^\dagger \cdot \mathbf{G}(\mathbf{r}_n, \mathbf{r}_n; \omega_{n'}') \cdot \mathbf{d}_{n'}\right]. \quad (5)$$

The usual SE rate from a single dipole in a generalized medium, $\Gamma_a = \Gamma_{a,a}$, shows that the single dipole emission is proportional to the $\mathbf{d}_a$-projected LDOS as expected. To characterize the strength of the dipole-medium coupling, we introduce the enhanced SE factor or Purcell factor through $F_{\mathrm{P}} = \Gamma_a/\Gamma_a^0$, where Γ_a^0 is the rate for

a homogeneous medium. In addition, there is a possible dipole-dipole coupling term given by $\Gamma_{a,b}$, and since $\mathbf{d}_a$ and $\mathbf{d}_b$ are orthogonal for realistic QDs, this term is usually neglected if $\mathbf{G}$ is isotropic. However, as we show below, AVI effects are possible at certain locations, depending upon the nature of the dipoles and the field modes; we then exploit such coupling effects to demonstrate a number of striking effects.

(*a*) Consider the case of coupled right- and left-CP dipoles, $\mathbf{d}_a = \frac{1}{\sqrt{2}}(\mathbf{d}_x + i\mathbf{d}_y) = \mathbf{d}^R$ and $\mathbf{d}_b = \frac{1}{\sqrt{2}}(\mathbf{d}_x - i\mathbf{d}_y) = \mathbf{d}^L$, coupled to a LP field mode, $\mathbf{E}_k = \alpha\mathbf{e}_k^x + \beta\mathbf{e}_k^y$, where $\alpha^2 + \beta^2 = 1$. (*i*) If $\alpha = 1$, then $\Gamma_{a,b} = \Gamma_{a,a} = \Gamma_{b,a}$. (*ii*) If $\beta = 1$, then $\Gamma_{a,b} = -\Gamma_{a,a} = \Gamma_{b,a}$. (*iii*) If $\alpha = \beta = \frac{1}{\sqrt{2}}$, then $\delta_{a,b} = \Gamma_{a,a}/2 = \delta_{b,a}$. Remarkably, all three scenarios can be realized in both cavity and waveguide systems; indeed, the first two cases can be exploited to completely eliminate radiative decay, while the latter case is causes by a dipole-dipole induced Lamb shift. (*b*) Next, consider LP dipoles, $\mathbf{d}_a = \mathbf{d}_x$ and $\mathbf{d}_b = \mathbf{d}_y$, coupled to an arbitrarily polarized field mode, $\mathbf{E}_k = \alpha\mathbf{e}_k^x + \beta\mathbf{e}_k^y e^{i\phi}$; here we find that dipole-dipole coupling is optimized when $\alpha = \beta = \frac{1}{\sqrt{2}}$, with $\phi = 0$, again yielding $\Gamma_{a,b} = \Gamma_{a,a} = \Gamma_{b,a}$; in this case, clearly one does not necessarily have to invoke the language of an AVI-induced interference, since in this basis the Green function is isotropic.

Note that a C point is rather special; here there is no dipole-dipole coupling for orthogonal dipoles at the same location; however, generalizing to the case of two spatially separated dipoles in a waveguide, then one finds a rich variety of dipole-dipole coupling, e.g., for RC polarized dipoles at two C points, $\Gamma_{a,b} = 2\Gamma_{a,a}\cos[k_\omega(x_a - x_b)]$; $\Gamma_{b,a} = 0$, [16]; and for LP dipoles at two C points, then $\delta_{a,b} = \Gamma_{a,a}\sin[k_\omega(x_a - x_b)]/2 = \delta_{b,a}$.

Free-field evolution: modified vacuum dynamics. Consider exciton a excited, with exciton b in the ground state. For the QD dipoles, we assume equal resonance energies at $\omega_0/2\pi = 200$ THz with dipole strength $d = 50$ D, with $\mathbf{d}_a = \mathbf{d}_R$ and $\mathbf{d}_b = \mathbf{d}_L$. For simplicity we neglect pure dephasing associated with charge noise, and recent experiments [23] have shown that such rates can be in the KHz range. For the cavity system, we use numbers typical for PC systems [18], and allow Q to vary, with $\varepsilon_b = 13$ and $V_{\text{eff}} = 5 \times 10^{-20}$ m^3; and for the PC waveguide, we use $V_{\text{eff}} = 4 \times 10^{-20}$ m^3, $n_g = c/v_g = 50$ (group index), $a = 400$ nm. After solving the ME (Eq. 3), the populations are obtained from $n_{a/b}(t) = \langle\sigma_{aa/bb}(t)\rangle$.

Figure 2(a) shows the population dynamics with and without AVI when $\alpha = \beta = \frac{1}{\sqrt{2}}$ [case $a(iii)$]. We introduce here a new mechanism that to the best of our knowledge is unknown: a Lamb-shift mediated dipole-dipole interaction between orthogonally polarized excitons, and the amount of population transfer is quite significant. While a decays faster, exciton b becomes excited and also decays radiatively. Next, we consider case $a(i)$ [or case (*b*) with LP dipoles]. The panels (b-d), show,
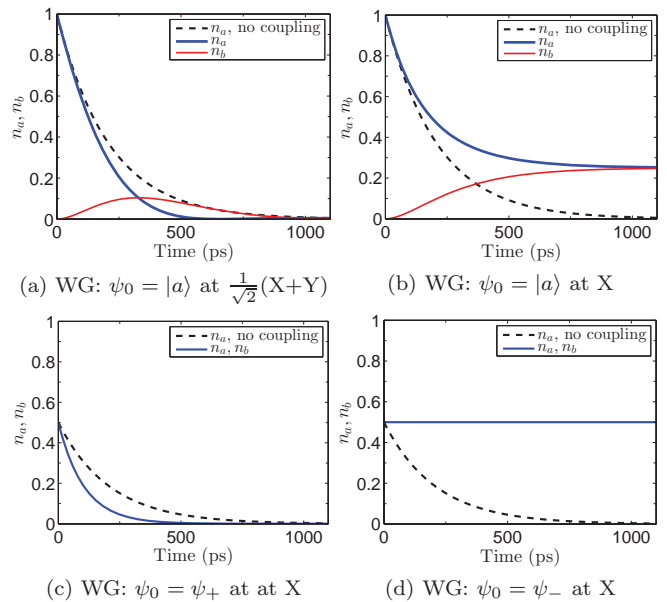

FIG. 2: (a-b) Free field evolution of a QD two-dipole system with an initially excited QD population inside a slow light waveguide, where (a) is at the $\frac{1}{\sqrt{2}}(\text{X+Y})]$ point and (b) is at the X point. Exciton a (blue thick) is initially excited and the AVI causes QD b (red thin) to be excited. The population decay without the AVI is shown in black dashed. In case (b), the system forms a pure state consisting of a linear combination of Bell states ψ_- and ψ_+. (c) Free field evolution with the system in the symmetric state, ψ_+, showing superradiance. (d) Evolution with an antisymmetric state, ψ_-, which stays in a pure excited state in the long time limit.

respectively, the decay from excited state a excited, and when we start the system in the antisymmetric and symmetric Bell states: $\psi_\pm = \frac{1}{\sqrt{2}}[|a\rangle|g\rangle \pm |b\rangle|g\rangle]$. In (b), the system evolves into a linear combination of $\psi_\pm$, and in (c) we see perfect super-radiance (double the single exciton decay rate); in (d), we completely suppress the radiative decay and evolve into a pure state, with no long lived decay, i.e., an optically dark state. For the rest of the paper we consider a QD at the X point, i.e., case $a(i)$. With regards to the corresponding enhanced SE rates, the Purcell factor in the waveguide, $F_\text{P} \approx 32$; and for the $Q = 1000$ cavity, $F_\text{P} \approx 109$—which are quite modest.

CW-pumped entanglement dynamics and population trapping. Next we look at the situation where one of the QD excitons is coherently pumped, e.g., with an external laser source, and the initial field is vacuum with the QD in the ground state. Normally this would be very difficult to do with spatially coupled dots in the near-field, but since the dipoles here are orthogonal one can selectively excite only one dipole (or both) with the appropriate pump field polarization. In Fig. 3(a), we consider the case where only exciton a is pumped in a waveguide, which shows good population coupling and a fidelity to project onto the state ψ_-, defined as F_-. In (b), the waveguide system is now excited antisymmetrically, where $\Omega_a = -\Omega_b$, and this turns out to be the most

(a) WG: Ω_a at X

(b) WG: Ω_{anti} at X

(c) Cavity: Ω_a at X
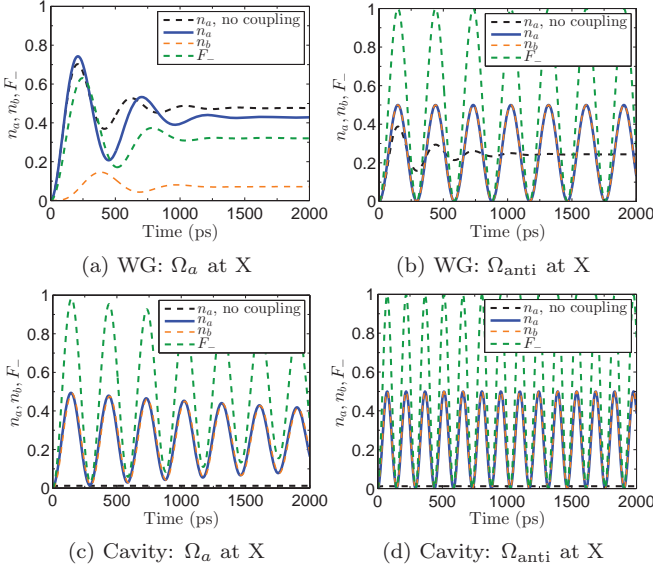
(d) Cavity: Ω_{anti} at X

FIG. 3: Examples of a coherently pumped QD two-dipole system. (a) WG (waveguide): Exciton a (blue solid) is pumped with $\Omega_a = 0.01$ meV cw driving field, and the AVI causes QD b (red dashed) to be excited. (b) Both excitons are pumped with $\Omega_{a/b} = \pm 0.01$ meV ($\approx 3.7\Gamma_a$). For the cavity (c-d), we use $Q = 3000$, and $\Omega_0 = 0.02$ meV ($\approx 0.06\Gamma_a$). The green dashed curve shows the fidelity of being in the state $\psi-$, which clearly exhibits perfect Rabi oscillations with no radiative decay.

(a) Q=3000: Ω_a=10 μeV

(b) Q=3000: $\Omega_{a/b}$=$\pm$10 μeV

(c) Q=500: Ω_a=180 μeV

(d) Q=3000: $\Omega_a = 0.2 \mu$eV

FIG. 4: Incoherent spectra (Mollow triplets) from exciton-a (blue solid) and exciton-b (red - dashed); the result for only 1 QD exciton is shown in the (black) thin dashed line. All results are at the X point in a cavity, and the vertical magenta lines indicate the single exciton dressed-state resonances. (a) $Q = 3000$ cavity with $\Omega_a = 10\,\mu$eV. (b) $Q = 3000$ cavity with $\Omega_{a/b} = \pm 10\,\mu$eV. (c) $Q = 500$ cavity with $\Omega_a = 180\,\mu$eV. (d) $Q = 3000$ cavity with $\Omega_a = 0.2\,\mu$eV.

striking case: we observe the formation of infinite coherent Rabi oscillations, and a complete suppression of the radiative decay; in this regime, we have created a population trapping state which has been studied extensively for multi-level atom systems [24–26]. Next we display the $Q = 3000$ cavity case in (c-d), and find similar trends, but now even case (c) shows a significant reduction of the radiative decay with only a excited; notably in this case, the single exciton case hardly shows any oscillation at all (it is clearly in the weak field regime). Here we see a way to explore high field physics, even though the Rabi field is much smaller than the intrinsic radiative decay rate of a single exciton. Note that for a Y point [case $a(ii)$], the the trapping solution is simply $\Omega_a = \Omega_b$, which yields the same trapping state.

To better explain the creation of a population trapping state, we have analyzed the optical Bloch equations from the ME, which reduce to two simple equations: $\dot{\rho}_{aa} = i\Omega_0 2\rho_{ga}$ and $\dot{\rho}_{ga} = i\Omega(1 - \rho_{aa})$, with $\rho_{ab} = -\rho_{aa}$, $\rho_{ga} = -\rho_{gb}$, $\rho_{bb} = \rho_{aa}$. These clearly mimic the coherent optical Bloch equations for a 2-level atom, but with a factor of two difference in the population term. Thus, the radiative decay processes cancel by virtue of the AVI-induced coherence, and population trapping occurs.

CW-pumped Mollow triplets, nonuplets and singlets. One of the most striking experimental signatures of high-field cw driven two-level systems is the Mollow triplet [27], which results from transitions between the field-driven dressed states. Recently the Mollow
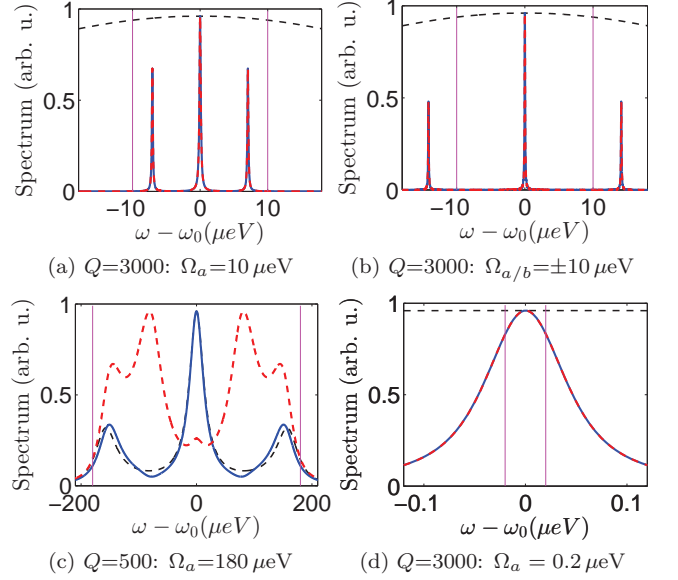
triplet in QD systems has been observed in a number of QD cavity systems [28–30]. Using Eq. (3) and the quantum regression theorem, the incoherent spectrum emitted from each QD exciton, n, is obtained from [22] $S_0^n(\omega) = \lim_{t\to\infty} \text{Re}[\int_0^\infty d\tau(\langle\sigma_{ng}(t+\tau)\sigma_{gn}(t)\rangle - \langle\sigma_{ng}(t)\rangle\langle\sigma_{gn}(t)\rangle)e^{i(\omega_L-\omega)\tau}]$, where we assume the detector is aligned with the corresponding polarization and we ignore additional filtering effects associated with light propagation from the QD to the detector (though these effects can be included [31]). We also consider the case where the QD excitons are directly pumped with an effective Rabi field, otherwise they will scale with Q and n_g if pumped through the cavity mode and PC waveguide mode, respectively.

Figures 4(a-b) show the Mollow triplet for the cavity case above, with one and two coherent fields, which demonstrate how the Mollow peaks are sharpened and clearly resolved, even though we are not in the Mollow regime ($\Omega \ll \Gamma_a$, cf. the broad black dashed spectrum from a single exciton.). Indeed, in the latter case, we have added a pure dephaing rate of 0.2 μeV, otherwise the peaks are infitesimally sharp. The next two panels show examples of some striking physics: (c) shows how to observe more than three spectral peaks, as we are now dealing with a dressed triplet of states, which yields 9 resonances, 5 of which are degenerate, so 5 resolvable peaks can be seen in general; similar peaks have been predicted for V-type 3-level atom when the dipole mo-

ments are nearly parallel [26]. While (d) demonstrates how to excite a single subnatural resonance, which has applications for producing single photon sources [14].

Conclusions. We have introduced several practical QD systems that can yield substantial dipole-dipole coupling between orthogonal dipoles within the same QD, through carefully nanoengineering the photonic AVI effects. We have also shown how to exploit such physics for generating a population trapping state and demonstrated the consequences of these states for exploring high field physics, such the Mollow triplet regime, with relatively weak fields. A wide range of other quantum optical effects should be accessible in this regime, including the possibility of exploring cavity-QED effects with cavities that are nominally in the weak coupling regime. Moreover, our formalism can easily be extended to multiple QDs, e.g., for use in chiral spin networks [32].

[1] G. S. Agarwal, Phys. Rev. Lett. **84**, 5500 (2000).
[2] G. xiang Li, F. li Li, and S. yao Zhu, Phys. Rev. A **64**, 013819 (2001).
[3] P. K. Jha, X. Ni, C. Wu, Y. Wang, and X. Zhang, Phys. Rev. Lett. **115**, 025501 (2015).
[4] L. Sun and C. Jiang, Opt. Exp. **24**, 7719 (2016).
[5] S. Axelrod, M. K. Dezfouli, H. M. K. Wong, A. S. Helmy, and S. Hughes, arXiv:1606.06957 (2016).
[6] P. Lodahl, S. Mahmoodian, and S. Stobbe, Rev. Mod. Phys. **87**, 347 (2015).
[7] A. J. Brash, L. M. P. P. Martins, F. Liu, J. H. Quilter, A. J. Ramsay, M. S. Skolnick, and A. M. Fox, Phys. Rev. B **92**, 121301 (2015).
[8] M. A. M. Versteegh, M. E. Reimer, K. D. J. ns, D. Dalacu, P. J. Poole, A. Gulinatti, A. Giudice, and V. Zwiller, Nature Communications **5**, 5298 (2014).
[9] M. Müller, S. Bounouar, K. D. Jöns, M. Glässl, and P. Michler, Nature Photonics **8**, 224 (2014).
[10] R. Trotta, J. Martin-Sanchez, J. S. Wildmann, anni Piredda, Reindl, C. Schimpf, E. Zallo, S. Stroj, J. Edlinger, and A. Rastelli, Nature Communications **7**, 10375 (2016).
[11] S. Sun, H. Kim, G. S. Solomon, and E. Waks, Nature Nanotechnology **11**, 539 (2016).
[12] R. Bose, T. Cai, K. R. Choudhury, G. S. Solomon, and E. Waks, Nat Photon. **8**, 858 (2014).
[13] D. Englund, D. Fattal, E. Waks, G. Solomon, B. Zhang, T. Nakaoka, Y. Arakawa, Y. Yamamoto, and J. Vu̇ckovic̀, Phys. Rev. Lett. **95**, 013904 (2005).
[14] C. Matthiesen, A. N. Vamivakas, and M. Atatüre, Phys. Rev. Lett. **108**, 093602 (2012).
[15] A. B. Young, A. C. T. Thijssen, D. M. Beggs, P. Androvitsaneas, L. Kuipers, J. G. Rarity, S. Hughes, and R. Oulton, Phys. Rev. Lett. **115**, 153901 (2015).
[16] I. Söllner, S. Mahmoodian, S. L. Hansen, L. Midolo, A. Javadi, G. Kiraanske, T. Pregnolato, H. El-Ella, E. H. Lee, J. D. Song, S. Stobbe, and P. Lodahl, Nature Nanotechnology **10**, 775 (2015).
[17] V. S. C. Manga Rao and S. Hughes, Phys. Rev. B **75**, 205437 (2007).
[18] P. Yao, V. S. C. Manga Rao, and S. Hughes, Laser Photon. Rev. **4**, 499 (2009).
[19] G. S. Agarwal, Phys. Rev. A **12**, 1475 (1975).
[20] H. T. Dung, L. Knöll, and D.-G. Welsch, Phys. Rev. A **66**, 063810 (2002).
[21] G. Angelatos and S. Hughes, Phys. Rev. A **91**, 051803 (2015).
[22] H. Carmichael, *Statistical Methods in Quantum Optics 1: Master Eq* (Springer, 1999).
[23] N. Somaschi, V. Giesz, L. D. Santis, J. C. Loredo, M. P. Almeida, G. Hornecker, S. L. Portalupi, T. Grange, C. Anton, J. Demory, C. Gomez, I. Sagnes, N. D. Lanzillotti-Kimura, A. Lemaitre, A. Auffeves, A. G. White, L. Lanco, and P. Senellart, Nat. Photon. **10**, 34 (2016).
[24] G. S. Agarwal, *Quantum Optics* (Springer, 1974) pp. 94–96.
[25] E. Paspalakis and P. L. Knight, Phys. Rev. Lett. **81**, 293 (1998).
[26] P. Zhou and S. Swain, Phys. Rev. Lett. **77**, 3995 (1996).
[27] B. R. Mollow, Phys. Rev. **188**, 1969 (1969).
[28] E. B. Flagg, A. Muller, J. W. Robertson, S. Founta1, D. G. Deppe, M. Xiao, W. Ma, G. J. Salamo, and K. Shih, Nature Physics **5**, 203 (2009).
[29] A. N. Vamivakas, Y. Zhao, C.-Y. Lu, and M. Atatüre, Nature Physics **5**, 198 (2009).
[30] S. Ates, S. M. Ulrich, S. Reitzenstein, A. Löffler, A. Forchel, and P. Michler, Phys. Rev. Lett. **103**, 167402 (2009).
[31] F. Hargart, M. Müller, K. Roy-Choudhury, S. L. Portalupi, C. Schneider, S. Höfling, M. Kamp, S. Hughes, and P. Michler, Phys. Rev. B **93**, 115308 (2016).
[32] H. Pichler, T. Ramos, A. J. Daley, and P. Zoller, Phys. Rev. A **91**, 042116 (2015).
[33] Note $\mathrm{Re}[\mathbf{G}(\mathbf{r}, \mathbf{r})]$ formally diverges but we work here with the transverse Green function ($\mathbf{G} = \mathbf{G}_{\mathrm{wg}}$, which has no divergence) and the vacuum contribution is included in the definition of $\omega_{a/b}$.